POLITECNICO DI TORINO
Repository ISTITUZIONALE

The contribution of fine-grained exposure data to flood risk assessment along the Niger River

Original
The contribution of fine-grained exposure data to flood risk assessment along the Niger River / Tiepolo, M., Housseini, M.I., Cannella, G., Katielliou, G.L., Ganora, D., Marmolejo Gutiérrez, A., Saretto, F., Tarchiani, V., Vesipa, R.. - In: NATURAL HAZARDS. - ISSN 1573-0840. - ELETTRONICO. - 122:(2026), pp. 1-31. [10.1007/s11069-026-08308-1]

Availability:
This version is available at: 11583/3013387 since: 2026-07-22T07:23:37Z

Publisher:
Springer

Published
DOI:10.1007/s11069-026-08308-1

Terms of use:

This article is made available under terms and conditions as specified in the corresponding bibliographic description in the repository

Publisher copyright

(Article begins on next page)

11 September 2026

Natural Hazards (2026) 122:554
https://doi.org/10.1007/s11069-026-08308-1

ORIGINAL PAPER

The contribution of fine-grained exposure data to flood risk assessment along the Niger River

Maurizio Tiepolo[1] · **Mohamed Ibrahim Housseini**[2] · **Giorgio Cannella**[1] · **Gaptia Lawan Katielliou**[3] · **Daniele Ganora**[1] · **Alejandro Marmolejo Gutiérrez**[1] · **Francesco Saretto**[1] · **Vieri Tarchiani**[1] · **Riccardo Vesipa**[1]

Received: 2 September 2025 / Accepted: 28 June 2026
© The Author(s) 2026

Abstract
The establishment of the Sendai Framework for Disaster Risk Reduction 2015–2030 prompted local governments to prepare flood risk assessments. However, within the rural contexts of low- and middle-income countries, such tools do not account for the details necessary for risk management. Limited data availability is the most frequently reported reason for such deficiencies. Moreover, flood exposure is particularly uncertain. This study aimed to overcome this obstacle through the use of fine-grained open-access information, local datasets, and ground truth data. Its novelty is the identification of flood-prone assets and the formulation of risk reduction measures. This approach was applied to a 58-km section of the Niger River upstream of Niamey. Notably, risk is considered the product of hazard and damage, expressed in monetary terms. On the basis of five hazard scenarios, hydraulic modelling was employed to determine the floodplain, which was then validated against Sentinel-2 satellite images. Buildings and crops were identified through visual interpretation of Google Earth satellite images and verified on the ground. Wells were located according to statistics from the Ministry of Hydraulics and Sanitation. The potential damage resulting from a flood with a 10-year return period was partitioned, with 57% attributed to crops and 43% to buildings. Horticulture alone accounted for 43% of the total damage. Half of the damage to buildings is concentrated in 13 settlements. Nine structural measures are recommended on the basis of the expected inundation depth.

Keywords Disaster risk reduction · Flood damage · Flood depth · Flood risk map · Horticulture · Hydraulic modelling

✉ Maurizio Tiepolo
maurizio.tiepolo@polito.it

[1] Politecnico di Torino, Turin, Italy

[2] Abdou Moumouni University of Niamey, Niamey, Niger

[3] Direction de la Météorologie Nationale, Niamey, Niger

Published online: 21 July 2026

1 Introduction

Since the 1960s, the magnitude, frequency, and duration of riverine floods have decreased globally (Liu et al. 2022), as has the number of resultant fatalities (Jonkman et al. 2024). However, in low- and middle-income countries (LMICs), the exposed population is more vulnerable (Tanoue et al. 2016), and floods are more deadly than they are elsewhere. Flood inequity has not decreased in recent years (Sauer et al. 2024). Within the Sendai Framework for Disaster Risk Reduction 2015–2030 (SFDRR) risk assessments are ranked at the top of the priorities for action (United Nations 2015). Satellite data open archives, global flood models (Ward et al. 2013), analysis techniques (Kaya et al. 2023; Kumar et al. 2023; Destefanis et al. 2025; Redondo-Tilano et al. 2025), technologies (Tao et al. 2024), and experimental methods (Abdulrahman et al. 2021) have facilitated the preparation of flood risk assessments (FRAs). Over the last decade, FRAs have increasingly relied on Earth observations, thereby becoming detached from communities and local knowledge (Bennett et al. 2024). As a result, the areas at risk are not delineated in detail. Sixty-eight percent of FRAs in LMICs still rely on satellite imagery with a spatial resolution of 30 m or more to identify exposure (Online Resource 1). Flood-prone assets are typically limited to land cover macroclasses, such as agricultural and developed areas. However, object-specific classification is rare (Glas et al. 2020; Diani et al. 2024). Moreover, critical flood-prone infrastructure (De Moel et al. 2009), such as boreholes and drinking water wells, has rarely been considered (Tiepolo et al. 2019). The monetary value of assets has been estimated for only buildings, rice, and maize (Shrestha et al. 2025). In summary, our understanding of exposure is limited (Grigg 2023). In half of the FRAs developed in LMICs, uncertainty in assets has constrained the determination of how to reduce risk (Online Resource 2).

Therefore, the problem lies in increasing our knowledge of exposure. This raises a research question with respect to how the use of more accurately defined and delineated flood-prone assets can improve FRAs. If this question is not answered, it is impossible to describe and localise flood prevention measures, assess whether such measures are effective, prepare long-term adaptation plans to face different climate scenarios, reveal the expected damage for each alert level of the early-warning system (EWS) (Najafi et al. 2024; Sidek et al. 2021), and organise effective recovery efforts after flooding. A better understanding of exposure can help to incorporate the risk dimension into planning and governance tools.

This study aimed to develop a detailed FRA using open-access and local information, as well as ground-truth data. We hypothesise that exposure can be quantified in detail even when information is scarce and that this process in turn can significantly contribute to risk management. An FRA was developed for a section of the Niger River upstream of the city of Niamey. This choice stems from the expectation of an increase in the occurrence of catastrophic floods (Aich et al. 2016) and the subsequent exposure of the area to flooding (Fiorillo et al. 2018; Massazza et al. 2021). In Niger, FRAs have been conducted primarily for individual rural settlements, towns, and cities (Tiepolo et al. 2019; 2023). Along the Niger River, attention has previously been given to the city of Niamey and the six local floods recorded in this area since August 2010 (Nouhou et al. 2025). This study is therefore novel for Niger, as it accounts for a large rural area instead of an urban area, and for all other contexts characterised by limited information availability, because it demonstrates the use of fine-grained exposure data in FRAs and risk management. This study can be replicated

along the 160 km upstream of the river, up to the border with Mali, since the river and the exposed assets are similar to those observed in the study section.

2 Materials and methods

2.1 Study area

The FRA was developed along a 58-km section of the Niger River, from its confluence with the Dargol tributary to the gates of Niamey. This stretch of the river is regularly inundated from June to September, as it receives water from the Dargol and Sirba rivers on its right bank, resulting in local (red) flooding. Conversely, rainfall in the upper basin in Guinea and Mali results in the occurrence of floods from November to February, referred to as Guinean floods (Massazza et al. 2021). The proximity of the study area to markets in Niamey and its accessibility via two paved national roads encouraged the development of commercial agriculture and the growth of rural settlements, which are not found along other stretches of the river in Niger (Fig. 1).

Four rural towns and 91 smaller settlements are located between the two national roads along the river. Of these, 36 settlements are distributed across 13 islands. The area is administratively part of the Bitikondji, Gothèye, Karma, Kourteye, and Namaro municipalities.

The hot, semiarid climate (BSh), as determinated according to the Köppen–Geiger classification, enables horticulture (1353 ha), hydro-agricultural developments (aménagements hydro agricoles in French or AHA) (1203 ha), and traditional rice fields, which provided sustenance for 72,000 inhabitants in 2012 (République2014). Elsewhere, rain-fed millet (*Pennisetum glaucum*) is the dominant crop, and is often cultivated in association with cowpeas (*Vigna unguiculata*) or peanuts (*Arachis hypogaea*).

2.2 Conceptual framework

This study focused on 40 fluvial FRAs in LMICs published after 2016 (Online Resources 1–2). Flood risk is the product of hazard and damage, expressed in monetary terms, according to a consolidated approach (Jonkman et al. 2008; De Moel et al. 2009; Merz et al. 2004; Tiepolo et al. 2021). FRA typically includes identifying risk reduction measures (IEC ISO 2009). We adopted a quantitative method (Birkmann and Welle 2015) that requires a combination of local and technical knowledge (Tiepolo and Braccio 2017). Hydraulic modelling was preferred over multicriteria analysis with the analytical hierarchical process technique (Shaibu et al. 2022; Mokhtari et al. 2023; Aichi et al. 2024) and morphometric analysis (Khalifa et al. 2023) because its ability to model flood scenarios that have not yet been observed and can therefore be integrated into the EWS. Local and central stakeholders helped define the methodology, provided information, described dynamics, interpreted the data, validated the remotely obtained results, and selected the measures to treat risk.

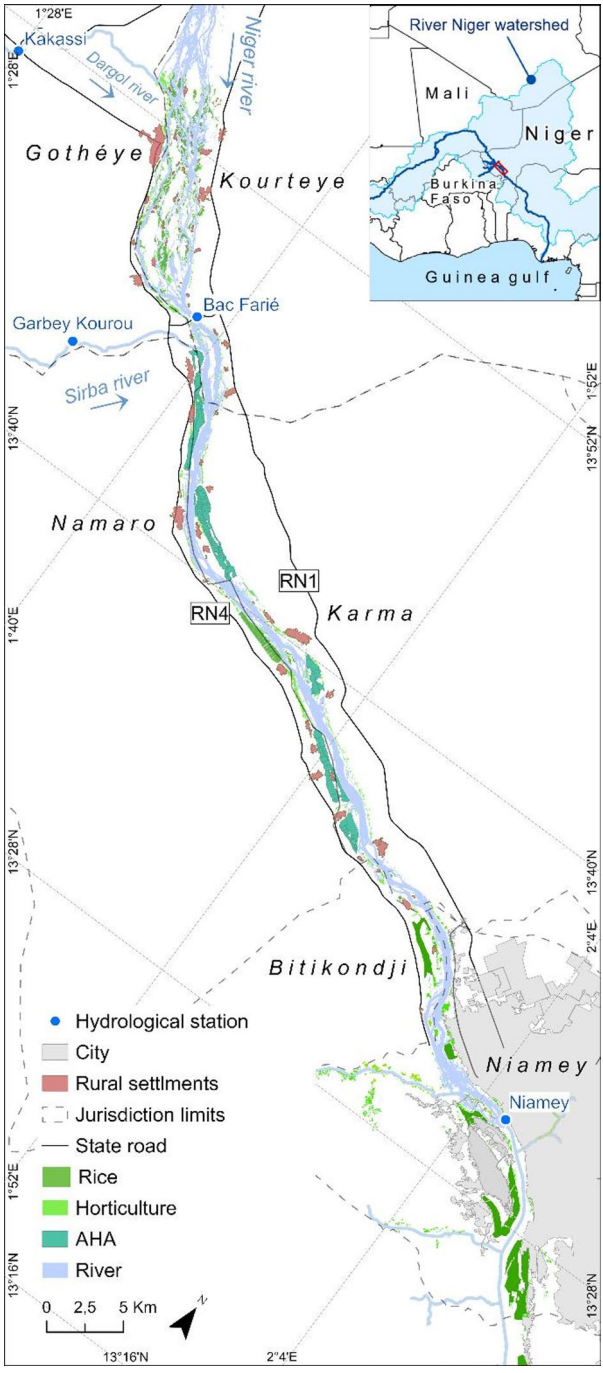

Fig. 1 Study area

Table 1 Summary of the hydrological data available

Station (River)	Data range	Years with less than 120 data	Source
Niamey (Niger)	1929–2025	1932–1933, 1937–1942, 2025	Niger Basin Authority and Hydraulic Directorate, corrected as in Tiepolo et al. (2025)
Garbey Kourou (Sirba)	1956–2025	1959–1961, 1992, 2000, 2004–2005	Tamagone et al. (2019), later updated with data from the Niger Basin Authority and Hydraulic Directorate (HD)
Kakassi (Dargol)	1957–2021	1957–1961, 1973, 1979–1981,1983–2003, 2005, 2021	Discharge data available from 1957 to 1982 (HD). From 2003 to 2021, data were reconstructed using hydrometric height data and the rating curve. Data from Niger Basin Authority and HD

Table 2 Hosking and Wallis (1997) homogeneity test results for the Garbey Kourou and Kakassi peak time series

H_1	H_2	H_3
0.03	0.02	0.58

$H_k < 1$: Acceptably homogeneous. $1 \leq H_k < 2$: Possibly heterogeneous. $H_k \geq 2$: Heterogeneous

2.3 Hazard

2.3.1 Hydrologic analysis

Flood hydrographs for the study area were estimated on the basis of daily time series of hydrological observations from the Garbey, Kourou, and Niamey stations (see Table 1). First, a flood frequency analysis was performed, as described by Tiepolo et al. (2025). This analysis involved detrending the annual maximum values, followed by fitting a generalised extreme value (GEV) distribution to estimate the daily peak flow for a given return period (RP). At the Niamey station, flood frequency analysis was performed separately for local and Guinean floods. Next, the shape of the hydrograph was modelled by calculating a dimensionless mean hydrograph for each station. The aforementioned was achieved by averaging all observed flood hydrographs, which were normalised by their yearly maximum values and centred on their peaks. Finally, we scaled the dimensionless hydrograph by multiplying it by the peak flow obtained from the frequency analysis for the required RP.

The data for Kakassi, exhibited significant gaps (Table 1), rendering them unsuitable for extreme value analysis. To overcome this issue, a time series for the Dargol Basin was defined by scaling data from the Sirba Basin (Garbey Kourou), after verifying similar behaviours of the two basins (Table 2). Flood hydrographs for Kakassi were thus calculated as:

$$Q^T_{Kakassi} = Q^T_{GarbeyKourou} * \alpha \tag{1}$$

with $\alpha = 0.186$ denotes the ratio between the areas of the Dargol Basin and the Sirba Basin.

Hydrographs were calculated separately for the months between June and October and between November and May, because of the two-peak behaviour of the Niger River. The hydrographs to be used in the hydraulic simulation process were defined according to Fig. 2, as follows:

$$Q^T_{Niamey}(d+1) = Q^T_{Upstream}(d) + Q^T_{Kakassi}(d) + Q^T_{GarbeyKourou}(d) \tag{2}$$

were d denotes a generic day of the season. Note that we considered a 1-day time lag in Niamey to account for the flood transit time between the upstream and downstream sections (this value was obtained from preliminary simulations). In practice, the hydrograph for the upstream section of the Niger reach for the Guinean flood can be defined as follows:

$$Q^T_{Upstream}\,(d) = Q^T_{Niamey}\,(d+1) - (\alpha+1)\cdot Q^T_{GarbeyKourou}\,(d) \tag{3}$$

; while for a local flood, the following applies:

$$Q^T_{Upstream}(d) = Q^T_{Niamey}(d+1)$$

where $Q_{GarbeyKourou} \approx Q_{Kakassi} \approx 0$.

2.3.2 Hydraulic simulation

The process of flood-extent mapping is based on fully two-dimensional, unsteady solutions of shallow-water equations (USWEs). A dedicated 2-D fluvial hydraulic mesh (Fig. 2) was first established by delineating the modelling domain and prescribing the hydraulic boundary conditions— including an inflow hydrograph at the upstream limit and outflow fixed-depth rating conditions at the downstream limit. Break lines were then inserted along material transitions or features where additional computational detail is needed. Each sub-polygon was subsequently tessellated into triangular elements whose size reflects the desired local resolution. Any polygons intentionally left unmeshed appeared as "holes" within the grid and represented suspected levee-protected zones, which were treated as no-flow areas. Upon completion, the mesh received (i) a high-resolution digital terrain model, (ii) spatially varying Manning roughness coefficients, and (iii) prescribed time-series boundary conditions. The solver advanced the USWE over every mesh element at each time step, thereby producing temporally evolving water-depth and velocity fields.

The analyses were conducted with BASEMENT (ETH Zurich), a free software simulation engine that can be coupled directly with the Quantum Geographic Information System (QGIS) for pre- and postprocessing purposes and can exploit graphics processing unit (GPU) acceleration on suitably configured virtual machines. The modelled reach — covering approximately 90 km of the Niger River, whose active channel widens from 0.6 to 3.5 km — requires a four-day hydrograph centred on the peak, thereby allowing the flood wave to enter, traverse, and exit the mesh while capturing the two days preceding and the two days following the crest.

The terrain input relies on the Shuttle Radar Topography Mission (SRTM) 30-m digital elevation model (DEM) and the Advanced Land Observing Satellite Phased Array L-band Synthetic Aperture Radar (ALOS PALSAR) 12.5 m DEM. These datasets were selected

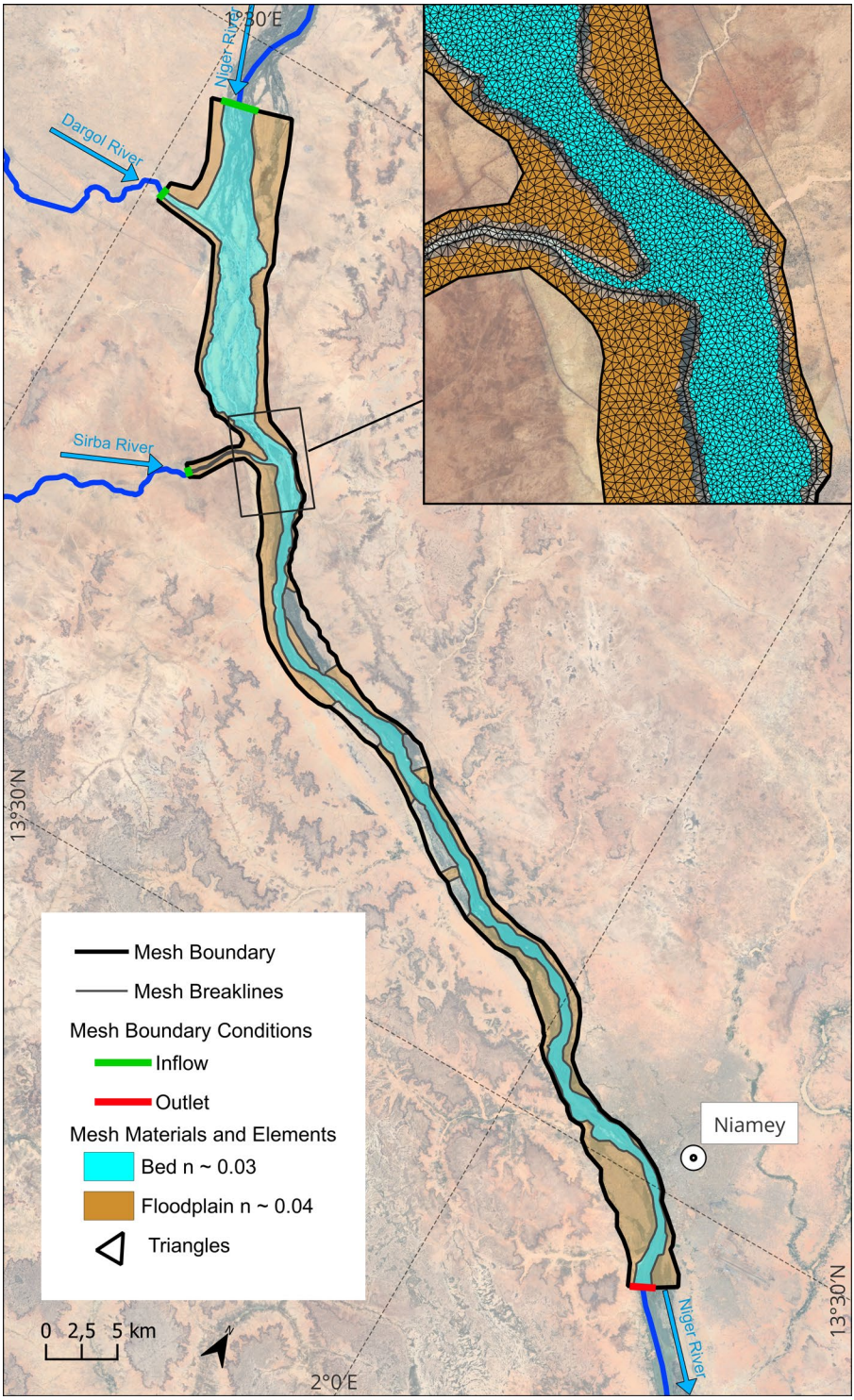

Fig. 2 Two-dimensional computational mesh

for their widespread use and global availability. Compared with other products, the SRTM results in smaller vertical error and more stable hydraulic performance levels (Santillan et al. 2016; Azizian and Brocca 2020). The ALOS PALSAR product was included to evaluate the benefits of finer spatial resolution in representing floodplain morphology. As radar sensors flatten open-water surfaces and do not capture the channel bathymetry, additional correction was needed along the river corridor. In the absence of surveyed bathymetric data, a discharge correction technique (Choné et al. 2018) was applied to adjust river elevations according to the discharge conditions at the time of DEM acquisition. A terrain correction technique was not adopted because it relies on quasi-one-dimensional assumptions that are inconsistent with the braided morphology observed along one-third of the study reach. In such multithread systems, imposing simplified cross-sectional geometries may introduce higher structural uncertainty than the bias associated with discharge-based correction.

Roughness values were derived from land cover inspections of this semi-arid environment, with values of $n = 0.030$ for the main channel and $n = 0.040$ for the largely bare areas or fallow floodplain. Notably, dense vegetation is largely absent.

Finally, synthetic design hydrographs representing RPs of 2, 5, 10, 30, and 100 years were routed through the model to generate depth-extent maps for damage appraisal and the formulation of corresponding risk reduction measures.

2.3.3 Sensitivity analysis

A first-order sensitivity analysis was performed on the RP100 inundation maps to quantify the extent to which vertical uncertainty in the DEM may affect the extent of the inundation. We applied ± 1 m vertical shifts to the DEM and measured the resulting change in inundation width along 10 representative cross-sections. The width was quantified using (i) the full inundated width and (ii) the sum of the subchannels.

2.3.4 Hazard map validation

The hazard map was validated on the basis of two flood inundation edges, derived from Sentinel-2 images processed via the modified normalised difference water index (MNDWI). The two images were acquired on 20 August 2024 and 16 February 2025, during the last local and Guinean flood peaks, respectively. Four flood simulations were generated with the BASEMENT model using the SRTM and ALOS PALSAR DEMs as inputs, along with discharge values for the two flood peaks. Flood inundation edges were derived from satellite images, and the hydraulic model was then converted from raster to polygon (vector) features to calculate the surface areas of the intersection and union between boundaries. For each scenario, the model performance with the two DEMs was quantified via the following index, which reflects the coincidence between the two sets of results (Horritt and Bates 2002)

$$F = (Smod \cup Sobs)/(Smod \cap Sobs)\,100 \tag{5}$$

where *Smod* is the simulated inundated surface area, and *Sobs* denotes the observed inundated surface area based on the MNDWI in the Sentinel-2 image. The *F* values range from

0 to 100%, indicating conditions ranging from no to complete coincidence between the model-predicted and satellite-derived inundated areas.

2.4 Damage

An accurate damage estimate should be object-specific. This requires knowledge of building types and their footprints, the extent of the most commonly grown crops, and their value. The Global Human Settlement Layer and Cropland Extent datasets cannot be used for this purpose because they rely on Sentinel imagery with 10-m spatial resolution (Schiavina et al. 2025), which impedes assets from being recognised and measured. Consequently, crops and buildings in April 2024 were identified via visual photointerpretation of images accessible on Google Earth (GE) platform with a spatial resolution of less than one metre. The shape and average dimensions of crops and buildings are shown in Fig. 3.

For land cover, class accuracy was assessed using 50 independent validation points interpreted according to the rules shown in Fig. 3 on the GE images of April 2024. The overall accuracy of 0.90 confirmed the reliability of the classification.

The identified crops were then classified according to the field morphology (cultivation pattern and size). Twenty-four fields were randomly sampled and visited during the flood peak on 16 February 2025 (Fig. 4).

Agricultural extension officers verified the crops and inundation edges (Tiepolo et al. 2025). The damage function of rice crops was expressed in the number of days of submer-

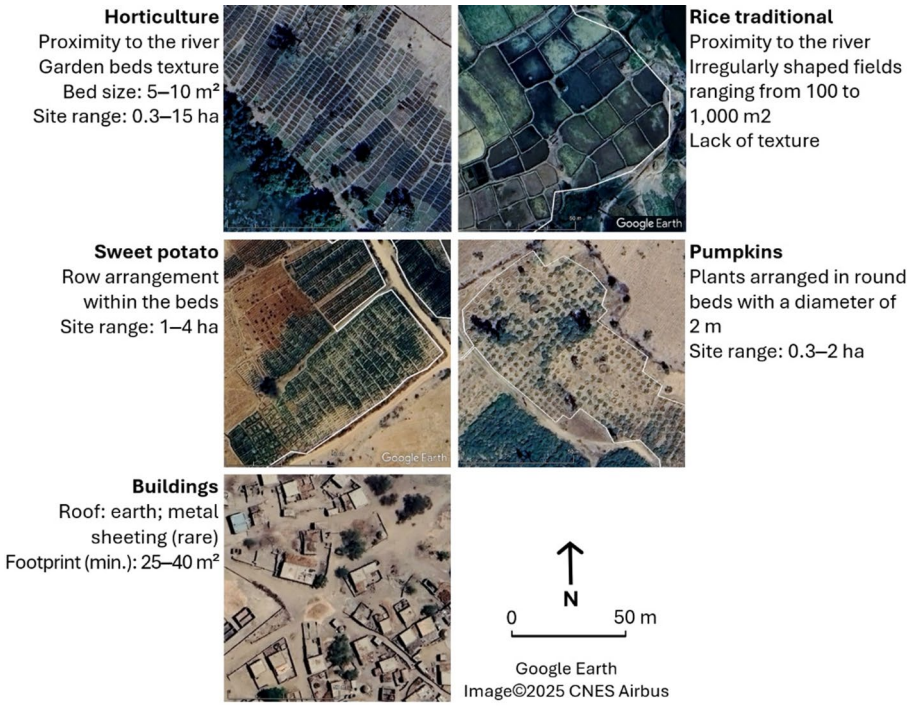

Fig. 3 Crops and buildings characteristics for visual photo interpretation of very high-resolution images from April 2024, available on GE

Fig. 4 Inspection of crops, February 16, 2025

sion/crop growth stage (Shrestha et al. 2016; Rahman et al. 2020), depending on the phenological stage (Tiepolo et al. 2025). The potential benefits of flooding, including additional crops and fuel savings for irrigation, were found to be null.

The levees protecting AHAs were considered floodproof. The damage to agriculture was calculated on the basis of the average yields of individual crops, as estimated by the Regional Chamber of Agriculture, the National Network of Agricultural Chambers, and on the basis of crop prices recorded by the Information System on Rural Markets (SIMA). With respect to buildings, the type of construction, water depth, and duration were considered. Overall, the built-up environment is characterised by single-storey adobe houses and rare buildings constructed of durable materials. Notably, adobe houses possess no door threshold. The long-term persistence of Guinean floods caused the total or partial collapse of affected buildings. The damage to buildings was estimated by applying the compensation recognised in recent public works in Niger (République 2024) (Table 3).

Data on georeferenced wells and boreholes were acquired from the statistics service of the Ministry of Hydraulics and Sanitation.

Table 3 Flood-prone asset substitution or restoration value as of February 2025

Asset	Action	Yield	Price at Gothèye			Reference
		T/ha	Euro/T	Euro/ha	Euro/unit	
Rice traditional	Substitution	3–5	706	2824		République (2025a)
Horticulture		–	–	8000		République (2025b)
Cassava		30	210	6300		
Okra		20	440	8200		
Onions		25	380	9500		
Pumpkings		25	326	8150		Issiakou et al. (2022)
Sweet potatoes		29	26–34	870		Chambre (2018), Safietou (2024)
Mais		5–7	410	2460		République (2012), (2025a)
Sorgho		2–2.5	460	1035		Kimba et al. (2025)
Adobe house 40 m^2		–	–	–	1520	République (2024)
Well	Desanding, disinfection	–	–	–	305	Hydraulics and Sanitation Ministry
Borehole		–	–	–	610	

2.5 Risk

The risk level was determined as the probability of flooding multiplied by the values of the exposed (i) adobe houses, (ii) wells, (iii) traditional rice, (iv) horticulture in mid-February 2025, (v) cereals and (vi) pulses in mid-August 2024.

2.6 Risk reduction

The risk reduction measures were initially selected on the basis of the inundation depth. These measures were then presented, discussed, and selected during a meeting with 16 stakeholders from four municipalities along the stretch of the river under study, the Ministry of Hydraulics and Sanitation, and the National Meteorological Directorate A participatory analysis was carried out to identify the Strengths, Weaknesses, Opportunities and Threats (SWOT) for each measure. The measures were then prioritized based on the community's familiarity with them, the availability of free land on which to implement them, the availability of local labour and materials, their moderate cost, their low maintenance requirements, their acceptance by the community, and their compliance with current legislation (Fig. 5).

3 Results

3.1 Hazard

Compared with Guinean floods, local floods in recent years have resulted higher discharge rates and stages (Fig. 6).

In the FRA, five local and Guinean flood scenarios were considered, with 2, 5, 10, 30, and 100-year RPs. According to the analysis described in Sect. 2.3.1, the river discharge

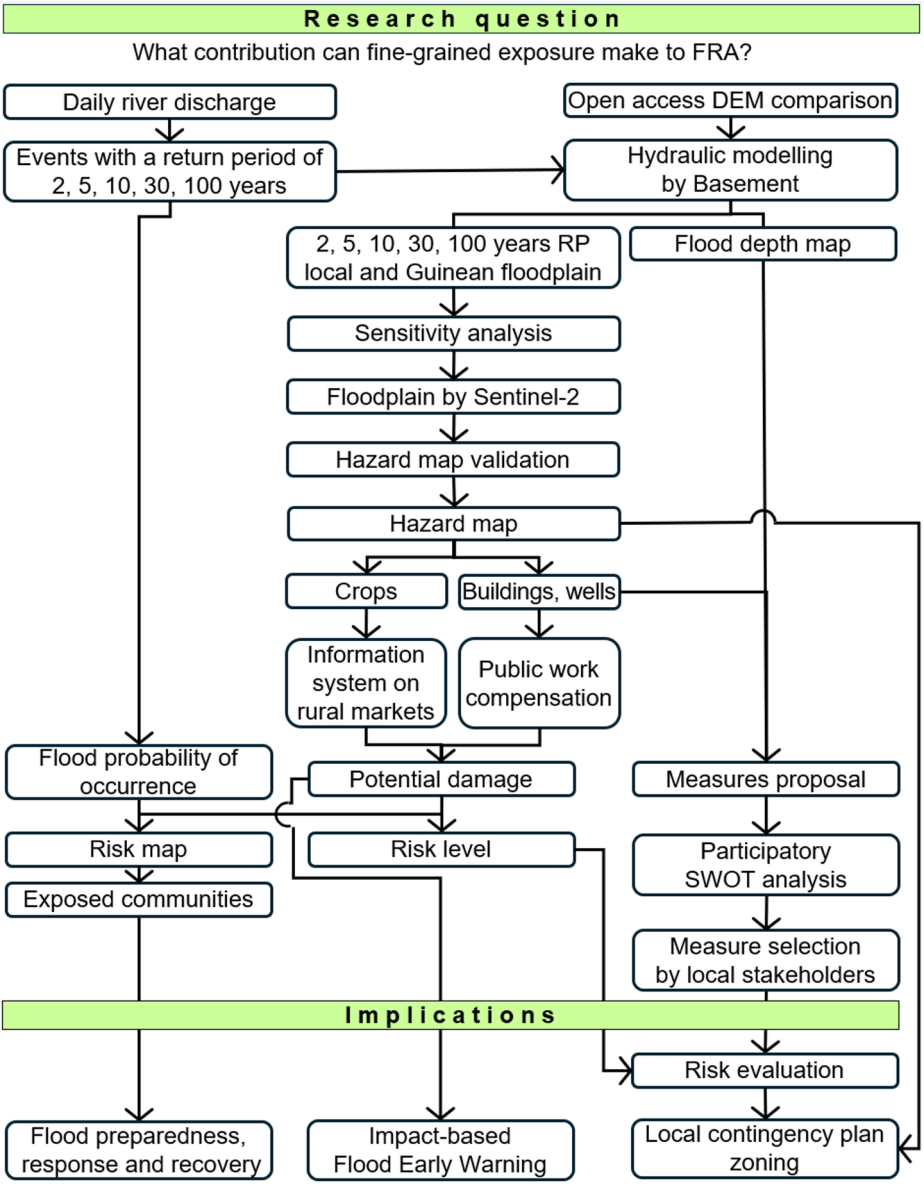

Fig. 5 Methodological flowchart

reached 1920, 2217, 2394, 2637, and 2858 m^3/s in Niamey during local floods and 1830, 2052, 2179, 2342, and 2486 m^3/s, respectively, during Guinean floods with RPs of 2, 5, 10, 30, and 100 years, respectively (Table 4).

According to the numerical hydraulic modelling results, the size of the floodplain area ranged from 119 to 128 km^2 (Fig. 7).

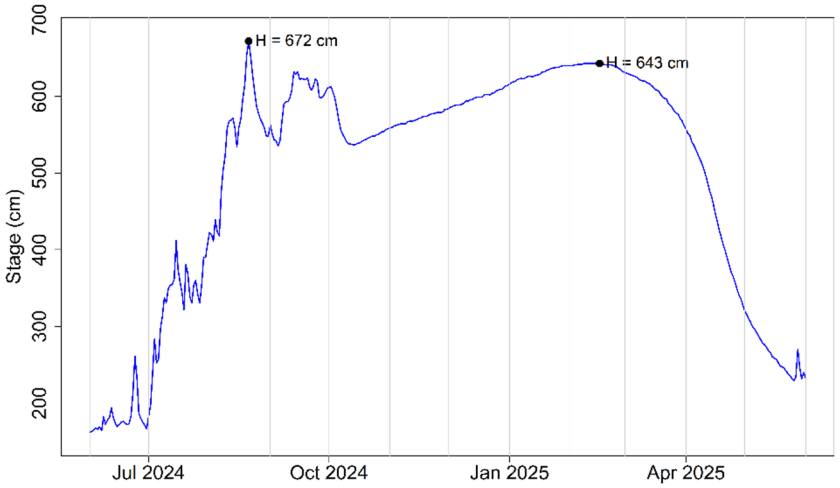

Fig. 6 Hydrograph of the Niger River at the Niamey gauge station from 2024–2025

Table 4 River discharge at the stations of interest for the selected return periods

Flood type	Return period	Probability	Station (River)		
			Niamey (Niger)	Garbey Kourou (Sirba)	Kakassi (Dargol)
	Years	%	m^3/s	m^3/s	m^3/s
Local	2	50	1920	733	137
	5	20	2217	939	175
	10	10	2394	1084	202
	30	3	2634	1319	246
	100	1	2858	1592	297
Guinean	2	50	1830		
	5	20	2052		
	10	10	2179		
	30	3	2342		
	100	1	2486		

The two types of floods entirely distinct manifestations. According to the reconstructed average hydrographs, local floods lasted two days on average at 99% of the peak, whereas the Guinean floods lasted one month at 99% of the peak. These distinct manifestations effect the resulting damage differently (Table 5).

3.1.1 Sensitivity

The average error in the full inundated width per unit of vertical error (± 1 m) varied between 6 and 8%, depending on Guinean of the type of flood (Guinean or local floods with an RP of 100 years). The error of the sum of subchannels varied between 15 and 18% (Table 6). When the full-width metric was used, only 1 of the 10 cross-sections indicated a relative increase greater than 25%. Via the use of the subchannel metric, 4 of the 10 cross-sections

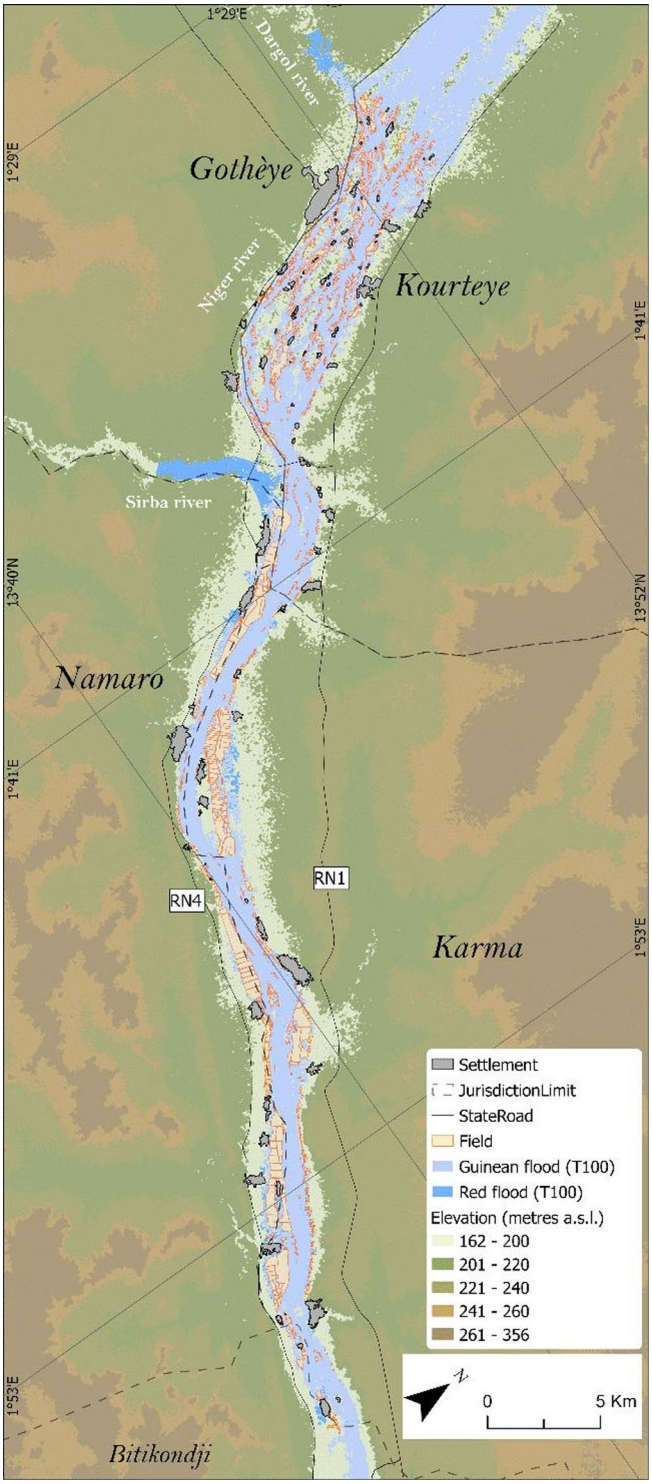

Fig. 7 Hazard map of local (red) and Guinean floods with a 100-year RP

Table 5 Flood average duration

Flood type	Flood duration (days)		
	Peak	99% of peak	95% of peak
Local	1	2	19
Guinean	1	27	53

Table 6 Mean horizontal error of the width of the modelled flood with an RP of 100 years per unit of vertical error of the DEM

DEM vertical error	Modelled flood horizontal error			
	Guinean flood RP100		Local flood RP100	
	Full width %	Sub-channel %	Full width %	Sub-channel %
+1 m	–6	–17	–8	–18
–1 m	9	15	8	15

Table 7 Degree of coincidence of the SRTM and ALOS PALSAR DEMs with the Sentinel-2 image

Flood type	Coincidence of satellite-derived flooded area with	
	SRTM %	ALOS PALSAR %
Local	60	57
Guinean	53	50

showed a relative increase or decrease of more than 25%. These higher sensitivities correspond to flatter and/or multichannel morphologies, in which small vertical offsets translated into greater horizontal shifts in the inundation boundary.

3.1.2 Hazard map validation

The values of the coincidence index between the simulated and observed flood extents ranged from ~ 50–60% for the two DEMs and flood seasons (Table 7).

The relatively modest agreement was driven mainly by the river configuration between the Dargol and Sirba confluences. In that segment, the channel is split into several narrow branches. Because neither the 30-m SRTM grid nor the 12.5-m ALOS PALSAR grid adequately resolves these small channels, the models overpredicted inundation relative to the Sentinel-2 NDWI footprint, thereby increasing the union term in the Jaccard index and decreasing the overall score.

The SRTM DEM yielded slightly higher coincidence values during both seasons. Thus, this product was selected for the remaining simulations. Similar choices—favouring an SRTM DEM over the notably finer-resolution ALOS product—have been reported by Garrote (2022) and Kaya and Üneş (2024), both of whom indicated that the vertical error structure and hydro-conditioning of the DEM can outweigh the advantage provided by the nominal pixel size when evaluating datasets for 2-D flood modelling.

3.2 Damage

Local floods between the Dargol–Niger river confluence and Niamey could inundate 461–856 ha of irrigated crops, thereby excluding AHA, depending on an RP of 2 or 100 years.

Guinean floods could inundate between 733 and 889 ha of irrigated crops. Notably, Guinean flood, with a 10-year RP, could submerge 205 ha of horticultural sites with more than 1 m of water. Fifty-eight settlements with a total population of 57 thousand people were identified as flood-prone (République 2014). Depending on the flood magnitude, 573–1226 buildings could be affected by local floods and 1,260 to 1801 buildings could be affected by Guinean floods. The exposed gross floor area ranged from 22,942 to 49,669 m^2 for local floods and from 49,282 to 69,071 m^2 for Guinean floods (Fig. 8, Table 8).

Only one well was identified in the flood zone with a 10-year RP, while two wells were identified near the flood zone with a 100-year RP. A total of 90% of the potential damage was caused by local flood with a 30-year RP, and by a Guinean flood with a 10-year RP

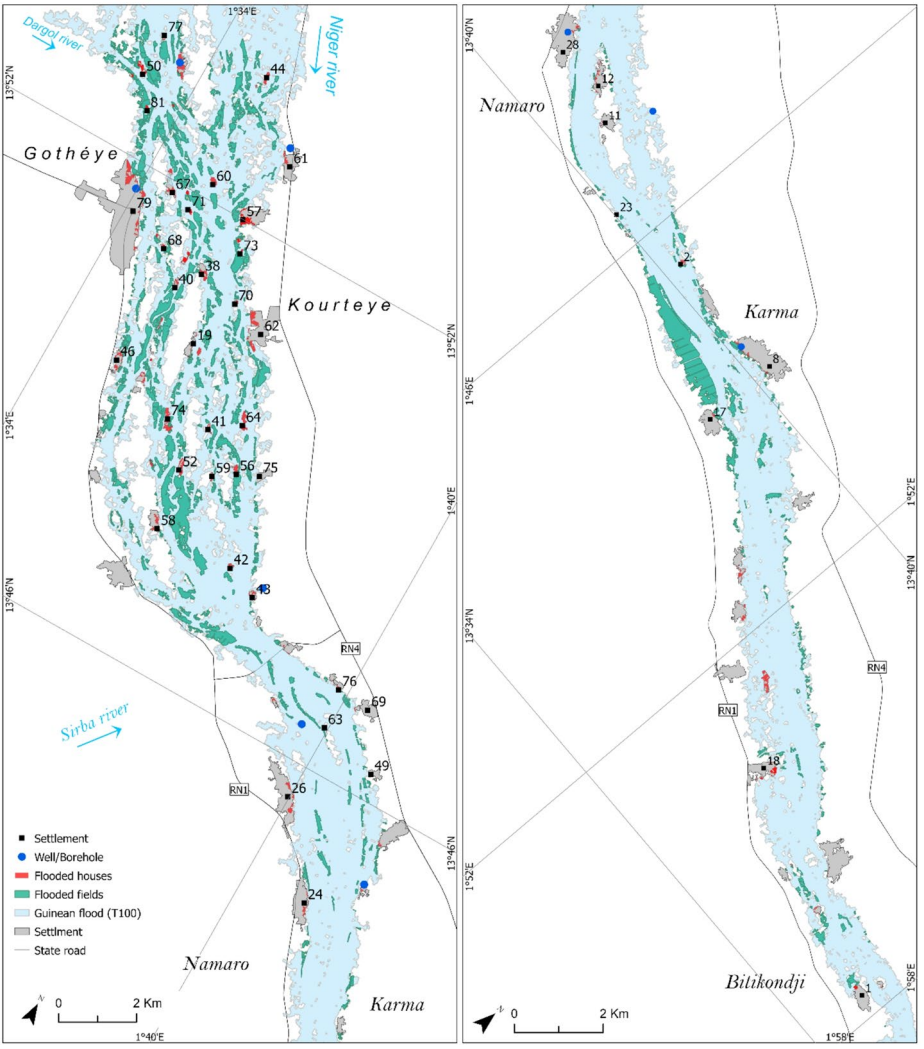

Fig. 8 Exposure map for Guinean floods with a 100-year RP in the Gothèye (left) and Karma (right) sectors

Table 8 Flood-prone buildings according to the flood type and RP

Flood type	Return period Years	Building	
		Number	m^2
Local	2	556	22,471
	5	682	26,903
	10	1132	44,314
	30	1408	57,647
	100	1165	47,350
Guinean	2	1226	47,980
	5	1424	54,290
	10	2152	83,739
	30	2141	84,471
	100	2405	94,245

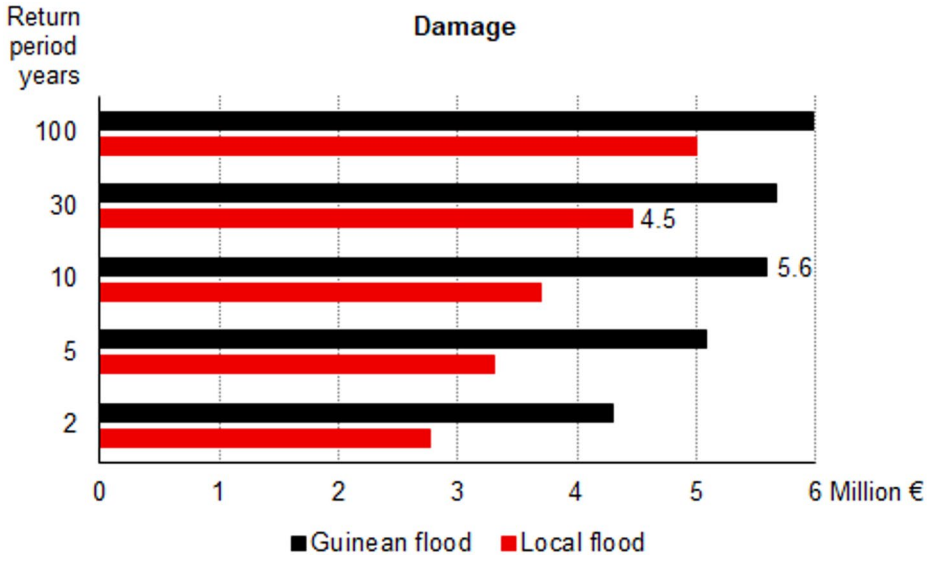

Fig. 9 Damage progress along the river Niger according to the flood type and RP

(Fig. 9). Half of the buildings at risk of flooding, in terms of the gross floor area, occurred in just thirteen settlements along the stretch of the Niger River between its confluence with the Dargol and Sirba Rivers, mainly on islands (Table 9, Online Resource 3). In Gothèye, Silboli, and Tcholondi, Guinean floods with a 100-year RP could affect 154, 117, and 150 buildings, respectively. Settlements on islands encompass minimal nonfloodable land available for further expansion (Fig. 10).

The potential damage amount ranged from 2.8 million to 5 million euros for local floods and from 4.3 million to 6 million euros for Guinean floods, depending on the RP. A total of 14–49% of these losses could be attributed to horticultural production losses from local floods, and 38–42% could be attributed to Guinean floods. The losses from traditional rice, sweet potato, and pumpkin cultivation varied between 14 and 60% because of local floods and between 13 and 17% because of Guinean floods. Building losses ranged from 26 to 37% of the total damage after local floods, reaching 45% in the case of Guinean floods. If we

Table 9 Gross floor area and water depth in the 13 settlements most exposed to Guinean floods with a 10-year RP

Settlement	Gross floor area floodable by water depth					
	All depths		0–0.5 m	0.5–1 m	1–2 m	>2 m
	m^2	%	%	%	%	%
All	65,143	100	21	26	26	26
Thirteen settlements	37,696	100	22	16	29	33
38 Damale	2042	100	0	49	34	17
79 Gothèye	5979	100	3	42	19	35
50 Kassani	2260	100	37	0	19	44
52 Kobadje	1738	100	0	31	64	5
56 Korsile	3129	100	0	24	21	55
57 Koulbagou	3103	100	34	0	17	50
60 Melle Goungou	2284	100	29	0	56	15
62 Sansane Haussa	2251	100	0	47	30	24
64 Silboli	3905	100	17	0	33	50
67 Sokole	1917	100	63	0	11	26
73 Tchirgni Koira	131	100	0	100	0	0
74 Tcholondi	6143	100	41	0	31	27
Village 42	2814	100	43	0	31	26

considered Guinean flood with a 10-year RP, 21% of the gross floor area of buildings would be inundated by less than 0.5 m of water, 26% would be inundated by between 0.5 and 1 m of water, 26% would be inundated by between 1 and 2 m of water, and another 26% would be inundated by more than 2 m of water.

3.3 Risk

Owing to the probability of occurrence and the potential damage expressed in monetary terms, the risk was always higher in the case of Guinean floods (2.2 million to 60,000 euros) than in the case of local floods (1.4 million to 50,000 euros). The risk decreased considerably with decreasing probability (Fig. 11).

Buildings accounted for between 27 and 33% of the overall risk level for local floods and between 37 and 39% for Guinean floods (Fig. 12, Online Resource 4).

3.4 Risk reduction

Risk reduction involves the implementation of nonstructural measures, such as hazard and exposure maps, a municipal emergency plan, and flood early warning. Structural measures depend on the expected inundation depth according to Guinean floods with a 10-year RP, which account for 90% of the total predicted damage. Two hundred five hectares of horticulture sites should be shifted to higher ground to prevent a potential 1-month period of inundation of crops by more than 1 m of water. This process involves upgrading irrigation systems with water storage basins and new wells. During local floods, buildings that could experience an inundation depth smaller than 0.5 m can be protected by the application of mobile barriers at the entrance and the placement of sandbags around the adobe walls. However, these measures are insufficient for Guinean floods at the same depth because of

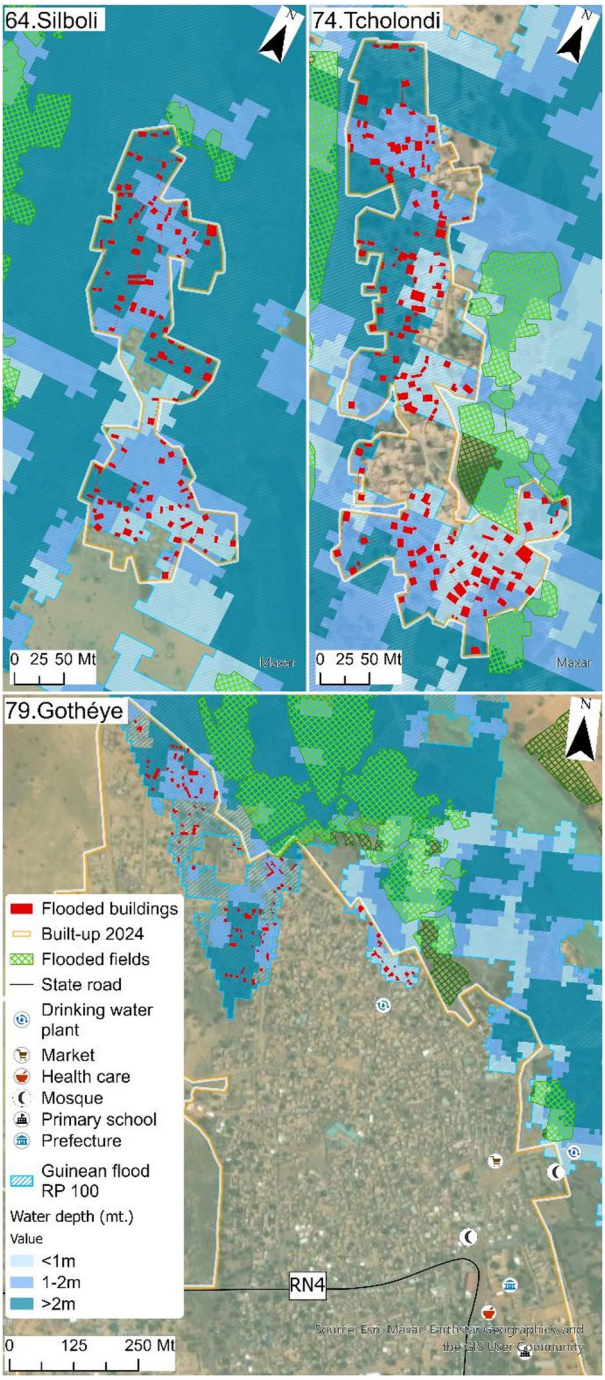

Fig. 10 Buildings susceptible to Guinean floods with a 100-year RP in Gothèye, Silboli, and Tcholondi

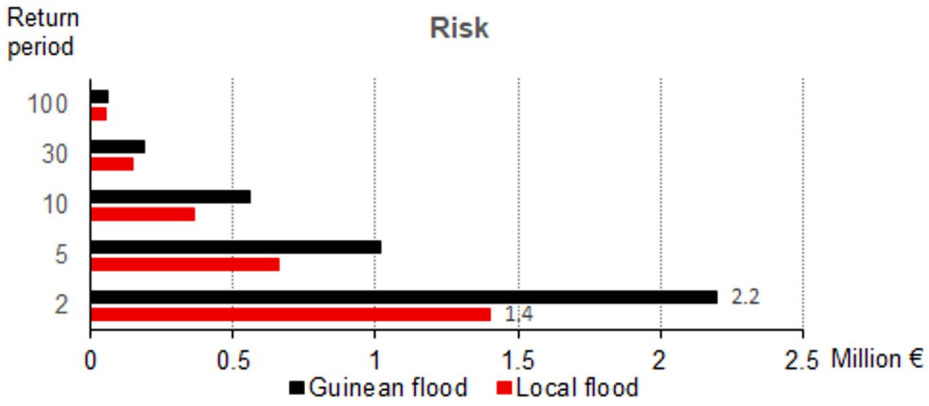

Fig. 11 Flood risk according to the flood type and return period

their duration. In this case, and for floods with water depths of 0.5–2 m, the construction of earthen levees is recommended. A total of 26% of the exposed gross floor area falls within this category. Moreover, a total of 26% could be exposed to depths greater than 2 m. In this case, resettlement constitutes the only viable solution. However, in Kassani, Kobadje, Silboli, and Tcholondi, no dry land remains for expanding settlements in continuity with developed areas, whereas in Damale, Koulbagou, Sokole, and Tchirni Koira, resettlement on dry land is still feasible (Fig. 13).

The magnitudes of the gross floor area and horticulture sites to be protected by specific measures are shown in Fig. 13.

FRAs should aim to estimate the cost of risk-reduction measures and compare them with the damage avoided by implementing these measures to determine whether the action is worthwhile. This step is impossible with SRTM and ALOS PALSAR DEMs because these products do not facilitate the accurate determination of protective levees around settlements or estimation of their cost. High resolution DEMs and ground inspections are necessary (Fig. 14).

4 Discussion

This study aimed to address the insufficient exposure data in FRAs for rural contexts in LMICs. The research question pertains to how the use of fine-grained exposure information can improve FRAs. We adopted open-access information, local datasets, and ground truth data to increase our understanding of the expected damage, risk reduction, local planning, and method refinement.

4.1 Expected damage understanding

Compared with local floods, Guinean floods generated greater risk and potential damage. A total of 90% of the potential damage could be caused by a Guinean flood with a 10-year RP. Guinean floods with a 2-year RP resulted in the highest risk (2.2 million euros). The risk of flooding decreased for RPs of 5, 10, 30, and 100 years. This trend is consistent with

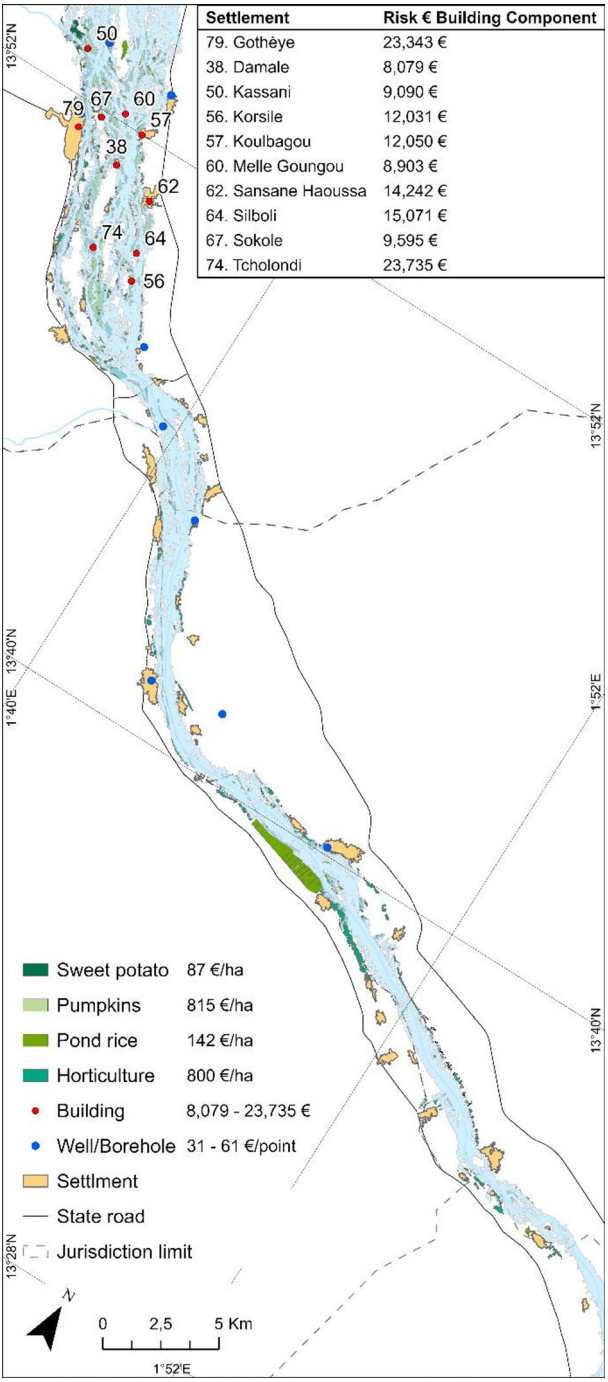

Fig. 12 Risk for Guinean floods with 10-year RP

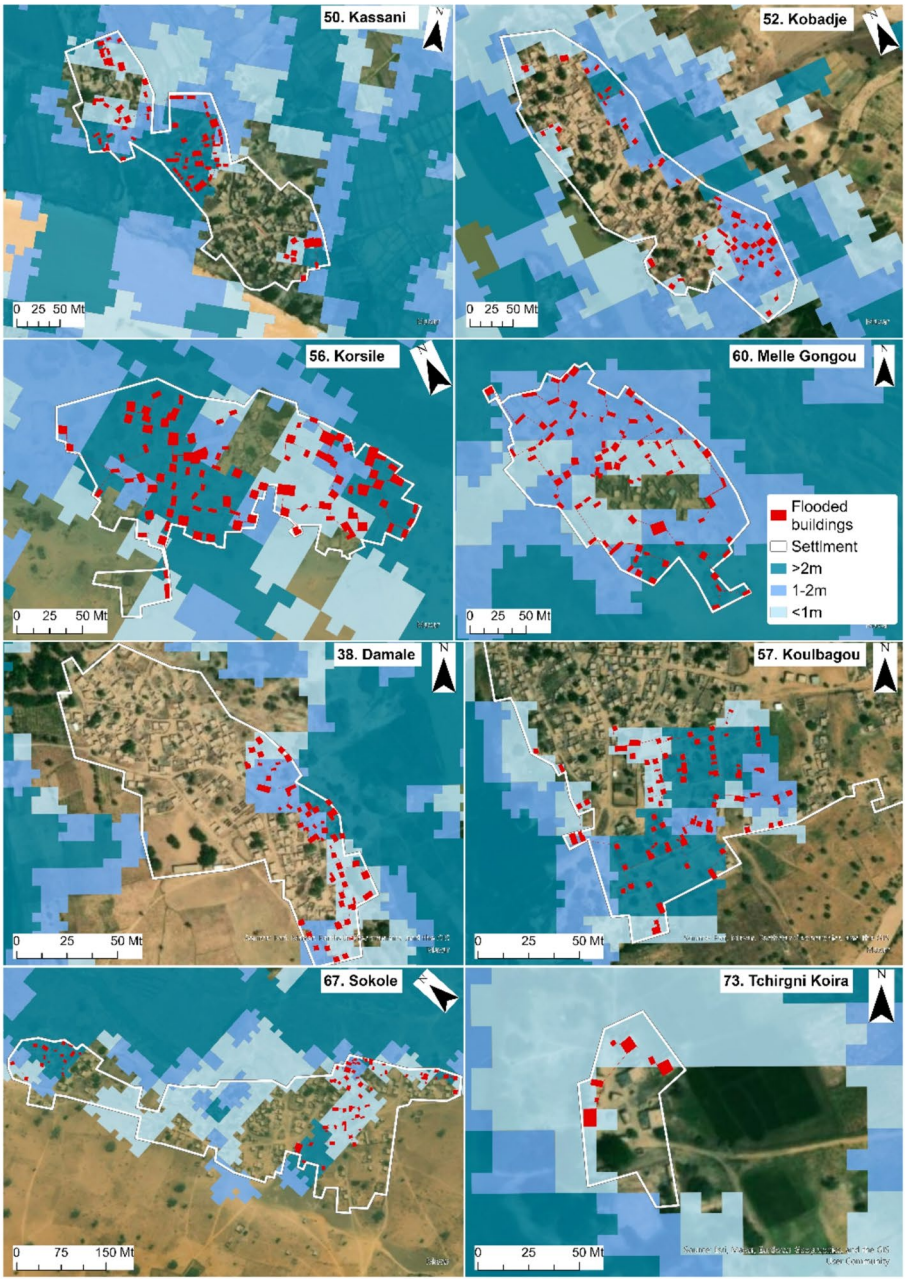

Fig. 13 Buildings likely affected by Guinean floods with a 10-year RP according to the water depth in Damale, Kassani, Kobadje, Korsile, Koulbagou, Melle Goungou, Sokole, and Tchirgni Koira

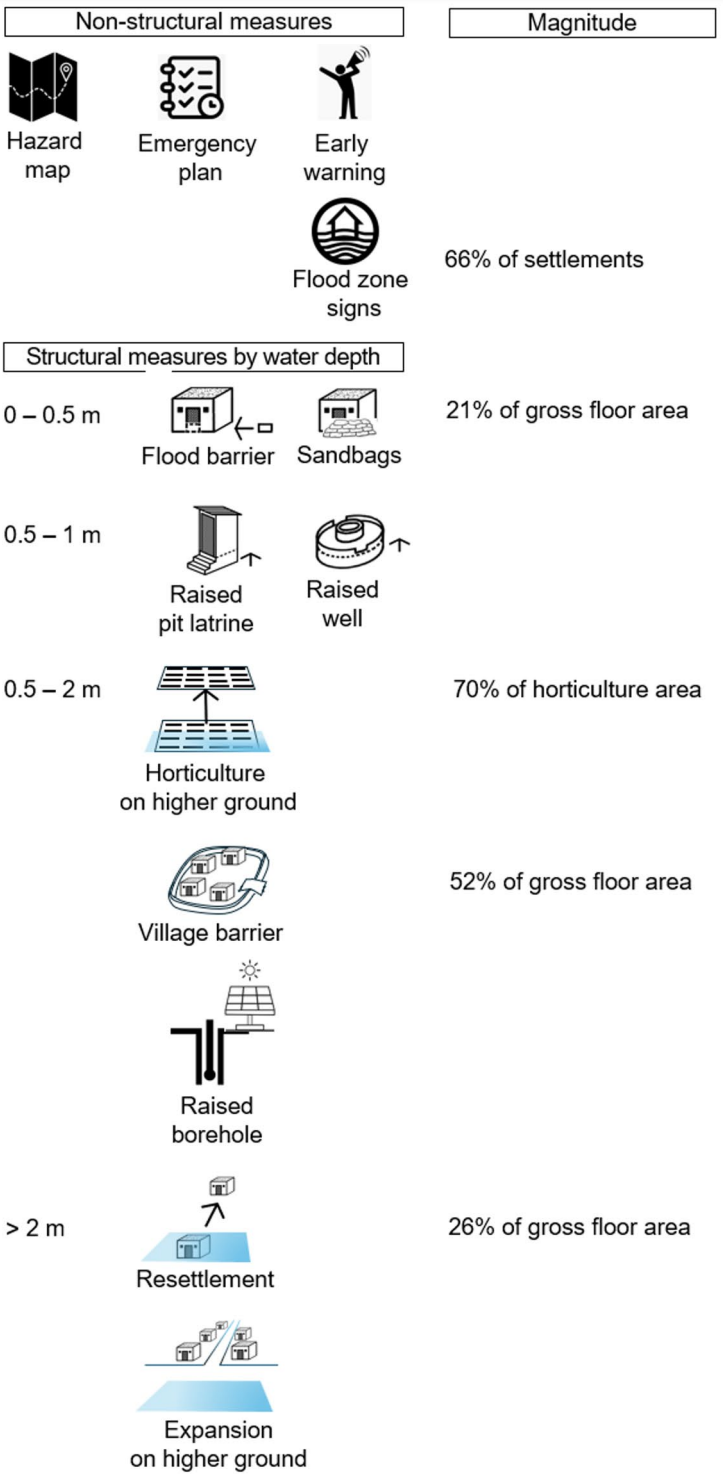

Fig. 14 Risk reduction measures according to the inundation depth

that observed by Mahmood et al. (2019) but is the opposite of the results obtained by Erima (2022) and Gunawan (2025). This finding is due to the location of irrigated fields near the river. The farther the flood leaves the riverbed, the fewer irrigated fields are encountered. Consequently, the multiplication of hazards by damage generates lower risk levels. This result suggests that local farmers can experience multiple catastrophic floods throughout their lifetimes.

Irrigated agriculture determined the risk level, confirming the observations of Nguyen et al. (2023) for other regions. Up to 43% of the risk level was attributed to horticulture, with a slightly higher value for the Guinean flood than for local floods. Flood-prone buildings, although significant in number and predominant within the housing stock of certain settlements, accounted for between 41 and 45% of the overall risk level, depending on the flood scenario.

4.2 Risk reduction

Half of the gross floor area susceptible to Guinean floods with a 10-year RP can be submerged by one metre of water that can persist for one month (Table 9). No door barriers or sandbags are sufficient to protect such buildings, since the adobe walls should also be protected for a long inundation time. A levee would be more suitable for protecting such buildings.

The seven settlements with the largest number of buildings exposed to floods with a 100-year RP are located on islands and cannot be expanded onto nonfloodable land. Expansion into the flood zone has already been observed in Niger by Galligari et al. (2020) and elsewhere (AL-Hussein et al. 2023; Fekete 2023; Monfared et al. 2024; Lamichhane et al. 2025). Thus, there is no local perception of hazards in areas where settlements expand. This finding suggests that flood hazard maps should be disseminated to local governments, and that the limit of the flood zone should be delineated to discourage future encroachment. These recommendations are not found in the literature (Online Resource 2).

Horticultural sites (205 hectares) likely to be covered by 1 m of water for 1 month after the Guinean floods with a 10-year RP should be shifted to higher ground. This choice obviously depends on land ownership, soil quality, and the availability of irrigation resources. Horticulture has rarely been considered in the literature on FRAs (Nguyen et al. 2023), which focuses only on rice (Shrestha et al. 2020; Syldon et al. 2024; Sharma et al. 2025).

The proposed measures are intended to be implemented within flood-prone areas to provide short- to medium-term protection for at-risk communities and local governments. Nature-based solutions (Acreman et al. 2021) designed to significantly reduce local floods in semi-arid regions are effective in the long term. In the medium River Niger, they should be implemented in the basin of its tributaries, outside the jurisdictions of riparian local governments and often in Burkina Faso and Mali.

In this FRA, the expected damage was linked to the National Alert Code of Niger (République 2019), in which the yellow (first) alert level is triggered for floods with a 2-year RP, the orange alert level involves floods with a 5-year RP and the red level pertains to floods with a 10-year RP. The responsibility for alerting is shared among civil protection, regions, districts, and municipalities, depending on risk extent and level. The message for each alert level should target the threatened settlements, and outline the types of assets exposed, and the actions to implement. This step is critical (Tarchiani et al. 2024; Syed et al. 2021; Shres-

tha et al. 2021) and should be defined in collaboration with the exposed communities (Tarchiani and Grey 2025).

4.3 Local planning

The FRA maps (Fig. 6, 9, and 12) and related data (Supplementary Information) may serve as the core of a geodatabase to support emergency and local development plans. Further information from sensors, hydraulic simulations, remote sensing, and crowdsourced mapping could be integrated (Samansiri et al. 2022). Floodplain mapping by inundation depth facilitates the identification of potentially affected infrastructure for evacuation and relief distribution. Moreover, inundation depth mapping enables the definition of the activities that should be prohibited and permitted in each zone. The identification of settlements and individual assets exposed to local and Guinean floods is crucial for ensuring effective prevention, preparedness (shelters), response (evacuation), and postflood recovery (damage assessment) in emergency plans. These FRA features are unusual in LMICs.

4.4 Method refinement

This study contributes to flood and damage modelling, one of the most widely employed methods in FRAs (Pinos et al. 2022). Recent studies have aimed to estimate the effects of climate change on flood-prone areas (Petiangma et al. 2025). We estimated flood damage on the basis of discharge data, both observed and modelled, including potential discharges resulting from climate change or variability. The FRA was therefore designed to be linked to the EWS. To achieve these results, we developed a microscale analysis whose results were recomposed at the mesoscale. Land cover global datasets cannot be used for damage modelling, because of their low resolution (Schiavina et al. 2025). We used GE data and freely available local datasets on crop yields and prices. Contrary to expectations (McCallum et al. 2016; Qadir et al. 2016), voluntary geographic information was almost nonexistent. We therefore involved the agricultural extension services of four riverine municipalities, which possess knowledge of the terrain and the ability to conduct local assessments necessary for validating modelled data at a lower cost than that associated with the use of remote sensing methods exclusively. This choice also offers an opportunity for providing a shared understanding of exposure (Bennett et al. 2024), empowerment and local ownership of the assessment (Calvo-Solano et al. 2024). Improving the quality of exposure data addresses a gap in flood risk assessment that global datasets have not yet managed to fill, particularly in rural areas of low- and middle-income countries.

4.5 Limitations

The most important limitation of this study is that it does not provide up-to-date information on the population exposed to flooding. This information would support humanitarian logistics (shelters and distribution of humanitarian kits). The Copernicus Global Human Settlement Layer or NASA's Gridded Population of the World, which is sometimes used for this purpose, cannot satisfy the needs of FRAs because of its low resolution (0.25–1 km grid) and infrequent updates. The fifth national population census of Niger, expected to release its first results in 2026, will fill this gap.

5 Conclusions

According to the midterm review of the implementation of the SFDRR (United Nations 2023), the number of risk assessments increased after 2015. However, FRAs for the rural contexts of LMICs provide insufficient details to support risk management. This research focused on the contribution of fine-grained exposure data to FRAs. We addressed this question on the basis of high-resolution satellite data, local datasets, and ground-truth information.

Our results revealed that Guinean floods are more catastrophic than local floods are because of their duration and the value of the seasonal crops affected. Moreover, buildings have been constructed in areas exposed to Guinean floods with a 10-year RP and a depth exceeding 2 m. Half of the exposed gross floor area at risk of flooding is concentrated in just 13 settlements. These findings suggest that the flood hazards associated with rapidly developing rural settlements are not perceived locally, thereby confirming the usefulness of hazard and exposure maps in preventing damage. The nature and location of exposed assets facilitated the formulation of 9 structural and 4 nonstructural measures to reduce flood risk.

This FRA is novel in its fine-grained asset identification and its proposed risk-reduction measures for individual settlements on the basis of the inundation depth.

Many FRAs now rely almost exclusively on satellite information and have become detached from communities. This approach offers solutions for contexts where conducting field activities has become unsafe. However, the case of the Niger River demonstrates that satellite information is insufficient to assess risk and its treatment. The resolution of open-access DEMs and hydrological information is inadequate and requires improvement in local datasets and the integration of local knowledge.

Future research could focus on (i) population data from the 2025 census for each flood-prone settlement, to contribute to preparedness, response, and recovery; (ii) expected damage between Kakassi and Farie hydrographic stations, Farie and Karma hydrographic stations, Karma and Niamey hydrographic stations, to contribute to the establishment of an impact-based EWS; and (iii) DEMs with higher resolution than that of the SRTM and ALOS PALSAR products, to quantify the proposed measures and evaluate flood risk. It would be desirable for the results of these studies to be incorporated into a geodatabase to update the FRA as potential damage patterns change over time.

The initial hypothesis regarding the feasibility of FRAs, even in contexts with little information, was partially confirmed. We demonstrated that, even in LMICs, more accurate FRAs can be developed when they are based on local knowledge.

Author contributions Maurizio Tiepolo, Daniele Ganora, and Riccardo Vesipa designed the study. Mohamed Housseini Ibrahim collected data on river discharge, wells, and boreholes, and described the site. Daniele Ganora and Francesco Saretto developed the hydrological analysis approach. Maurizio Tiepolo and Giorgio Cannella contextualised the study from the perspective of the FRA literature, collected and processed the asset information, and generated all the maps. Gaptia Lawan Katiellou characterised the local climate and supervised the field work. Alejandro Marmolejo Gutierrez and Riccardo Vesipa developed the hydraulic model. Vieri Tarchiani ensured the operability of risk level classification and its mapping into the flood EWS. All the authors commented on previous versions of the manuscript and approved the final manuscript.

Funding Open access funding provided by Politecnico di Torino within the CRUI-CARE Agreement. This study was funded by the Italian Agency for Development Cooperation, SLAPIS project, AID 12487.

Declarations

Conflict of interest The authors have no relevant financial or non-financial competing interests to disclose.

Open Access This article is licensed under a Creative Commons Attribution 4.0 International License, which permits use, sharing, adaptation, distribution and reproduction in any medium or format, as long as you give appropriate credit to the original author(s) and the source, provide a link to the Creative Commons licence, and indicate if changes were made. The images or other third party material in this article are included in the article's Creative Commons licence, unless indicated otherwise in a credit line to the material. If material is not included in the article's Creative Commons licence and your intended use is not permitted by statutory regulation or exceeds the permitted use, you will need to obtain permission directly from the copyright holder. To view a copy of this licence, visit http://creativecommons.org/licenses/by/4.0/.

References

Abdulrahman S, Bwambale J (2021) A review on flood risk assessment using multicriteria decision making technique. World Water Policy 7:209–221. https://doi.org/10.1002/wwp2.12058

Acreman M, Smith A, Charters L, Tickner D, Opperman J, Acreman S, Edwards F, Sayers P, Chivava F (2021) Evidence for the effectiveness of nature-based solutions to water issues in Africa. Environ Res Lett. https://doi.org/10.1088/1748-9326/ac0210

Aich V, Liersch S, Vetter T, Fournet S, Andersson JCM, Calmanti S, van Weert FHA, Hattermann FF, Paton EN (2016) Flood projections within the Niger River basin under future land use and climate change. Sci Total Environ 562:666–657. https://doi.org/10.1016/j.scitotenv.2016.04.021

Aichi A, Ikirri M, Ait Haddou M, Quesada-Román A, Sahoo S, Singha C, Sajinkumar KS, Abioui M (2024) Integrated GIS and analytic hierarchy process for flood risk assessment in the Dades Wadi watershed (central high Atlas, Morocco). Results Earth Sci 2:100019. https://doi.org/10.1016/j.rines.2024.100019

AL-Hussein AAM, Hamed Y, Bouri S, Hajji S, Aljuaid AM, Hachicha W (2023) The socio-economic effects of floods and ways to prevent them: a case study of the Khazir River basin, Northern Iraq. Water 15:4271. https://doi.org/10.3390/w15244271

Azizian A, Brocca L (2020) Determining the best remotely sensed DEM for flood inundation mapping in data sparse regions. Int J Remote Sens 41(5):1884–1906. https://doi.org/10.1080/01431161.2019.1677968

Bennett MM, Gleason CJ, Tellman B, Alvarez Leon LF, Friedrich HK, Ovienmhada U, Mathews AJ (2024) Bringing satellites down to Earth: six steps to more ethical remote sensing. Glob Environ Chang Adv 2:100003. https://doi.org/10.1016/j.gecadv.2023.100003

Birkmann J, Welle T (2015) Assessing the risk of loss and damage: exposure, vulnerability and risk to climate-related hazards for different country classifications. Int J Glob Warm 8:191–212. https://doi.org/10.1504/IJGW.2015.071963

Calvo-Solano O, Quesada-Román A (2024) Worldwide research trends and networks on flood early warning systems. GeoHaz 5:582–595. https://doi.org/10.3390/geohazards5030030

Chambre Régionale d'Agriculture de Dosso (2018) Fiche technico-économique pour la culture de la patate douce en saison sèche-froide. https://reca-niger.org/IMG/pdf/Fiche_technico_economique_patate_douce_CRA_Dosso_version_juin_2018docx.pdf, Accessed 8 July 2025

Chone G, Biron PM, Buffin-Bélanger T (2018) Flood hazard mapping techniques with LiDAR in the absence of river bathymetry data. E3S Web Conf. 40:06005. https://doi.org/10.1051/e3sconf/20184006005

de Moel H, van Alphen J, Aerts JCJH (2009) Flood maps in Europe–methods, availability and use. Nat Hazards Earth Syst Sci 9:289–301. https://doi.org/10.5194/nhess-9-289-2009

Destefanis T, Guliyeva S, Boccardo P, Fissore V (2025) Advancing flood detection and mapping: a review of earth observation services, 3D data integration, and AI-based techniques. Remote Sens 17:2943. https://doi.org/10.3390/rs17172943

Diani K, Hamza MH, Elbelrhiti H, Kacimi I, Faqihi FZ, Haghighi AT, El Amrani M, Hahou Y, Masmoudi L, Lahcen O, Alshehri F, Elhag M (2024) Flood risk assessment, a case study in an arid environment of Southeast Morocco. Open Geosci 16:20220607. https://doi.org/10.1515/geo-2022-0607

Erima G, Kabenge I, Gidudu A, Bamutaze Y, Egeru A (2022) Differentiated spatial-temporal flood vulnerability and risk assessment in lowland plains in Eastern Uganda. Hydrol Sci J 9:201. https://doi.org/10.3390/hydrology9110201

Fekete A (2023) Peri-urban growth into natural hazard-prone areas: mapping exposure transformation of the built environment in Nairobi and Nyeri, Kenya, from 1948 to today. Nat Hazards 119:859–882. https://doi.org/10.1007/s11069-022-05515-4

Fiorillo E, Crisci A, Issa H, Maracchi G, Morabito M, Tarchiani V (2018) Recent changes of floods and related impacts in Niger based on the ANADIA Niger flood database. Climate (Basel) 6:59. https://doi.org/10.3390/cli6030059

Galligari A, Giulio Tonolo F, Massazza G (2020) Floodplain settlement dynamics in the Maouri Dallol at Guéchémé, Niger: a multidisciplinary approach. Sustainability (Basel) 12:5632. https://doi.org/10.3390/su12145632

Garrote J (2022) Free global DEMs and flood modelling: a comparison analysis for the January 2015 flooding event in Mocuba city (Mozambique). Water 14:176. https://doi.org/10.3390/w14020176

Glas H, De Maeyer P, Merisier S, Deruyter G (2020) Development of a low-cost methodology for data acquisition and flood risk assessment in the floodplain of the river Moustiques in Haiti. J Flood Risk Manag 13:e12608. https://doi.org/10.1111/jfr3.12608

Grigg NS (2023) Comprehensive flood risk assessment: state of the practice. Hydrol 10:46. https://doi.org/10.3390/hydrology10020046

Gunawan WC, Javas J, Yosa IM, Suwarman R, Farid M, Adityawan MB (2025) Spatial modeling of high flood risk region in the Cikapundung River basin using HEC-RAS 2D model: enhancing regional mitigation planning. IOP Conf Ser Earth Environ Sci 1472:012038. https://doi.org/10.1088/1755-1315/1472/1/012038

Horritt MS, Bates PD (2002) Evaluation of 1D and 2D numerical models for predicting river flood inundation. J Hydrol 268:87–99. https://doi.org/10.1016/S0022-1694(02)00121-X

Hosking JRM, Wallis JR (1997) Regional frequency analysis: an approach based on L-moments. Cambridge University Press

IEC ISO (2009) International standard IEC/ISO 31010 Risk management: risk assessment techniques, Geneva (Switzerland) international electrotechnical commission

Issiakou DM, Ouanou A, Idi A, Mamadou K, Yayé Z (2022) Fiche technico-économique culture de la courge en hivernage. CRA Agadez. https://reca-niger.org/IMG/pdf/fte_courge_cra_agadez_decembre_2022.pdf. Accessed 8 July 2025

Jonkman SN, Bočkarjova M, Kok M, Bernardini P (2008) Integrated hydrodynamic and economic modelling of flood damage in the Netherlands. Ecol Econ 66:77–90. https://doi.org/10.1016/j.ecolecon.2007.12.022

Jonkman SN, Curran A, Bouwer LM (2024) Floods have become less deadly: an analysis of global flood fatalities 1975–2022. Nat Haz 120:6327–6342. https://doi.org/10.1007/s11069-024-06444-0

Kaya CM, Derin L (2023) Parameters and methods used in flood susceptibility mapping: a review. J Water Clim Change 14:1935–1960. https://doi.org/10.2166/wcc.2023.035

Kaya YZ, Üneş F (2024) Comparison of three different satellite data on 2D flood modelling using HEC-RAS (5.0.7) software and investigating the improvement ability of the RAS mapper tool. J Flood Risk Manag 18:e13046. https://doi.org/10.1111/jfr3.13046

Khalifa A, Bashir B, Alsalman A, Naik SP, Nappi R (2023) Remotely sensed data, morpho-metric analysis, and integrated method approach for flood risk assessment: case study of Wadi Al-Arish landscape, Sinai, Egypt. Water (Basel) 15:1797. https://doi.org/10.3390/w15091797

Kimba A and Delmas P (2025) Les variétés de semences améliorées disponibles dans l'Annuaire National 2025. Mil – sorgho – niébé – arachide. Réseau National des Chambres d'Agriculture du Niger. https://reca-niger.org/IMG/pdf/varietes_de_semences_certifiees_disponibles_2025_reca.pdf. Accessed 8 July 2025

Kumar V, Sharma KV, Caloiero T, Mehta DJ, Singh K (2023) Comprehensive overview of flood modeling approaches: a review of recent advances. Hydrology (Basel) 10:141. https://doi.org/10.3390/hydrology10070141

Lamichhane K, Karki S, Sharma K, Khadka B, Acharya B, Biswakarma K, Adhikari S, Kc R, Danegulu A, Bhattarai S, Regmi A, Subedi M, Bhattarai PK (2025) Unraveling the causes and impacts of increasing flood disasters in the Kathmandu valley: lessons from the unprecedented September 2024 floods. Nat Hazards Res 5:875–897. https://doi.org/10.1016/j.nhres.2025.04.001

Liu J, Feng S, Gu X, Zhang Y, Beck HE, Zhang J, Yan S (2022) Global changes in floods and their drivers. J Hydrol 614:128553. https://doi.org/10.1016/j.jhydrol.2022.128553

Mahmood S, Rahman A, Shaw R (2019) Spatial appraisal of flood risk assessment and evaluation using integrated hydro-probabilistic approach in Panjkora River Basin, Pakistan. Environ Monit Assess 191:573. https://doi.org/10.1007/s10661-019-7746-z

Massazza G, Bacci M, Descroix L, Ibrahim MH, Fiorillo E, Katiellou GL, Panthou G, Pezzoli A, Rosso M, Sauzedde E, Terenziani A, De Filippis T, Rocchi L, Burrone S, Tiepolo M, Vischel T, Tarchiani V (2021) Recent changes in hydroclimatic patterns over medium Niger River basins at the origin of the 2020 flood in Niamey (Niger). Water 13:1659. https://doi.org/10.3390/w13121659

McCallum I, Liu W, See L, Mechler R, Keating A, Hochrainer-Stigler S, Mochizuki J, Fritz S, Dugar S, Arestegui M, Szoenyi M, Laso Bayas J-C, Burek P, French A, Moorthy I (2016) Technologies to support community flood disaster risk reduction. Int J Disaster Risk Sci 7:198–204. https://doi.org/10.1007/s13753-016-0086-5

Merz B, Kreibich H, Thieken A, Schmidtke R (2004) Estimation uncertainty of direct monetary flood damage to buildings. Nat Hazards Earth Syst Sci 4:153–163. https://doi.org/10.5194/nhess-4-153-2004

Monfared AF, Ahmadi M, Derafshi K, Khodadadi M, Najafi E (2024) Urban development assessment in flood hazard areas using integrated HEC-RAS, SCS, and FAHP models: a case study of Pardisan settlement, Qom. Model Earth Syst Environ 10:5103–5120. https://doi.org/10.1007/s40808-024-02053-9

Najafi H, Shrestha PK, Rakovec O, Apel H, Vorogushyn S, Kumar R, Thober S, Merz B, Samaniego L (2024) High-resolution impact-based early warning system for riverine flooding. Nat Commun 15:3726. https://doi.org/10.1038/s41467-024-48065-y

Nguyen HD, Nguyen THT, Nguyen Q-H, Nguyen TG, Dang DK, Nguyen YN, Bui TH, Nguyen ND, Bui Q-T, Brecan P, Petrisor A-I (2023) Bottom-up approach for flood-risk management in developing countries: a case study in the Gianh River watershed of Vietnam. Nat Haz 118:1933–1959. https://doi.org/10.1007/s11069-023-06098-4

République du Niger, Ministère de l'agriculture et de l'élévage, INRAN (2012) Fiche descriptive de Nagode. https://reca-niger.org/IMG/pdf/Fiche_Descriptive_mais_hybride_Nagode_INRAN_2018.pdf, Accessed 8 July 2025

République du Niger, Institut National de la Statistique (2014) Répertoire national des localités (ReNaLoc), Niamey, INS. https://www.stat-niger.org/wp-content/uploads/renaloc/ReNaLoc_RGPH_2012.pdf

République du Niger (2019) Décret du Ministère de l'Intérieur, de la Sécurité Publique, de la Décentralisation et des Affaires Coutumières et Religieuses. Code d'alerte national; République du Niger: Niamey, Niger.

République du Niger, Ministère du Commerce et de l'Industrie, SIMA (2025b) Bulletin Mensuel Produits Agricoles 333. https://simaniger.net/download/bulletin-mensuel-des-produits-agricoles-n333-du-mois-de-fevrier-2025/. Accessed 8 July 2025

République du Niger, Ministère de Transports et de l'Equipement (2024) Plan d'actions de réinstallation (PAR) du tronçon Diffa-N'guigmi sur environ 35 kilomètres. Rapport provisoire, Niamey, Niger. https://www.bnee.ne/wp-content/uploads/2024/12/PICSN_PAR_Diffa_Nguigmi_RP.pdf. Accessed 9 June 2025

République du Niger, Ministère du Commerce et de l'Industrie. SIMA (2025a) Bulletin Hebdo Céréales 786 1. https://simaniger.net/download/bulletin-hebdo-cereales-n786-semaine-n8-du-mercredi-19-au-mardi-25-fevrier-202525/. Accessed 8 July 2025

Nouhou YD, Otache MY, Illiassou SA, Okunola OH, Okhimamhe AA, Nguyen TT (2025) Flood risk assessment and zoning for Niamey and Lokoja metropolises in Niger and Nigeria. Hydrol Sci J 12:17. https://doi.org/10.3390/hydrology12010017

Petiangma DM, Singh GG, Quesada-Román A, Hidalgo H, Blake S, Gonzalez A, McFarlin A, Collin R (2025) Climate change and flood susceptibility in Bocas del Toro, Panama: a multi-criteria spatial analysis approach. J Environ Manag 395:127741. https://doi.org/10.1016/j.jenvman.2025.127741

Pinos J, Quesada-Román A (2022) Flood risk-related research trends in Latin America and the Caribbean. Water (Basel) 14:10. https://doi.org/10.3390/w14010010

Qadir J, Ali A, ur Rasool R, Zwitter A, Sathiaseelan A, Crowcroft J (2016) Crisis analytics: big data-driven crisis response. J Int Humanit Action 1:12. https://doi.org/10.1186/s41018-016-0013-9

Rahman S, Di L (2020) A systematic review on case studies of remote-sensing-based flood crop loss assessment. Agricultura 10:131. https://doi.org/10.3390/agriculture10040131

Redondo-Tilano SA, Boucher M-A, Lacey J (2025) Emerging strategies for addressing flood-damage modeling issues: a review. Int J Disaster Risk Reduct 116:105058. https://doi.org/10.1016/j.ijdrr.2024.105058

Safietou FMC (2024) Evolution du prix de la patate douce pendant quatre ans (2020 à 2023) sur le marché de Katako à Niamey, Réseau National des Chambres d'Agriculture du Niger. https://reca-niger.org/IMG/pdf/note_prix_patate_douce_niamey_reca_2024.pdf. Accessed 8 July 2025

Samansiri S, Fernando T, Ingirige B (2022) Advanced technologies for offering situational intelligence in flood warning and response systems: a literature review. Water (Basel) 14:2091. https://doi.org/10.3390/w14132091

Santillan JR, Makinano-Santillan M (2016) Vertical accuracy assessment of 30-m resolution ALOS, Aster, and SRTM global DEMS over Northeastern Mindanao, Philippines. ISPRS Int Arch Photogramm Remote Sens Spat Inf Sci. https://doi.org/10.5194/isprsarchives-XLI-B4-149-2016

Sauer IJ, Mester B, Frieler K, Zimmermann S, Schewe J, Otto C (2024) Limited progress in global reduction of vulnerability to flood impacts over the past two decades. Commun Earth Environ 5:239. https://doi.org/10.1038/s43247-024-01401-y

Schiavina M, Melchiorri M, Mari Rivero I, Florio P, Freire S (2025) GHSL WUP projections data package 2025: public release GHS-WUP R2025, Publications office of the European Union, Luxembourg. https://doi.org/10.2760/2416436, JRC144209

Sharma AP, Fu X, Kattel GR, Adhikari TR, Hassan MA (2025) Appraising flood risk and inundation extent using GIS-aided 2D hydraulic modeling in Nepal Himalaya: a case of West Rapti River Basin. Model Earth Syst Environ 11:176. https://doi.org/10.1007/s40808-025-02356-5

Shrestha BB, Kwasaki A (2020) Quantitative assessment of flood risk with evaluation of the effectiveness of dam operation for flood control: a case of the Bago River Basin of Myanmar. Int J Disaster Risk Assess 50:101707. https://doi.org/10.1016/j.ijdrr.2020.101707

Shrestha BB, Okazumi T, Miyamoto M, Sawano H (2016) Flood damage assessment in the Pampanga River basin of the Philippines. J Flood Risk Manag 9:355–369. https://doi.org/10.1111/jfr3.12174

Shrestha MS, Gurung MB, Khadgi VR, Wagle N, Banarjee S, Sherchan U, Parajuli B, Mishra A (2021) The last mile: flood risk communication for better preparedness in Nepal. Int J Disaster Risk Reduct 56:102118. https://doi.org/10.1016/j.ijdrr.2021.102118

Shrestha A, McCrone A, Láng-Ritter J, Gautam S, Taka M, Varis O (2025) Bridging gaps, saving lives: integrating communities' voices and impact mapping into flood early warning systems in rural Nepal. Int J Disaster Risk Reduct 118:105238. https://doi.org/10.1016/j.ijdrr.2025.105238

Shuaibu A, Hounkpè J, Bossa YA, Kalin RM (2022) Flood risk assessment and mapping in the Hadejia River basin, Nigeria, using hydro-geomorphic approach and multi-criterion decision-making method. Water 14:3709. https://doi.org/10.3390/w14223709

Sidek LM, Basri H, Mohammed MH, Marufuzzaman M, Ishak NA, Ishak AM, Omar BZC, Osman S, Ramly S, Hassan MH (2021) Towards impact-based flood forecasting and warning in Malaysia: a case study at Kelantan River. IOP Conf Ser Earth Environ Sci 704:012001. https://doi.org/10.1088/1755-1315/704/1/012001

Syed MA, Shrestha MS, Khadgi V (2021) Last mile communication of multihazard early warning-a case study on Bangladesh. In: Pal I, Shaw R, Djalante R, Shrestha S (eds) Disaster resilience and sustainability. Adaptation for sustainable development. Elsevier, pp 725–765. https://doi.org/10.1016/B978-0-323-85195-4.00002-0

Syldon P, Shrestha BB, Miyamoto M, Tamakawa K, Nakamura S (2024) Assessing the impact of climate change on flood inundation and agriculture in the Himalayan mountainous region of Bhutan. J Hydrol Reg Stud 52:101687. https://doi.org/10.1016/j.ejrh.2024.101687

Tamagone P, Massazza G, Pezzoli A, Rosso M (2019) Hydrology of the Sirba River: updating and analysis of discharge time series. Water 11:156. https://doi.org/10.3390/w11010156

Tanoue M, Hirabayashi Y, Ikeuchi H (2016) Global-scale river flood vulnerability in the last 50 years. Sci Rep 6:36021. https://doi.org/10.1038/srep36021

Tao Y, Tian B, Adhikari BR, Zuo Q, Luo X, Di B (2024) A review of cutting-edge sensor technologies for improved flood monitoring and damage assessment. Sensors (Basel) 24:7090. https://doi.org/10.3390/s24217090

Tarchiani V, Bacci M (2024) The added value of the process in climate services co-production: lessons from Niger. Clim Serv 33:100435. https://doi.org/10.1016/j.cliser.2023.100435

Tarchiani V, Grey S (2025) Bridging the communication gap in agrometeorological services: enhancing the uptake and effectiveness for users in developing countries. Clim Serv 37:100531. https://doi.org/10.1016/j.cliser.2024.100531

Tiepolo M, Braccio S (2017) Local and scientific knowledge integration for multi-risk assessment in rural Niger. In: Tiepolo M, Pezzoli A, Tarchiani V (eds) Renewing local planning to face climate change in the tropics. Springer, Cham, Switzerland, pp 227–245. https://doi.org/10.1007/978-3-319-59096-7_11

Tiepolo M, Rosso M, Massazza G, Belcore E, Issa S, Braccio S (2019) Flood assessment for risk-informed planning along the Sirba River, Niger. Sustainability 11:4003. https://doi.org/10.3390/su11154003

Tiepolo M, Belcore E, Braccio S, Issa S, Massazza G, Rosso M, Tarchiani V (2021) Method for fluvial and pluvial flood risk assessment in rural settlements. MethodsX 8:101463. https://doi.org/10.1016/j.mex.2021.101463

Tiepolo M, Braccio S, Fiorillo E, Galligari A, Katiellou GL, Massazza G, Tarchiani V (2023) Participatory risk assessment of pluvial floods in four towns of Niger. Int J Disaster Risk Reduct 84:103454. https://doi.org/10.1016/j.ijdrr.2022.103454

Tiepolo M, Abraiz M, Bacci M, Baoua O, Belcore E, Cannella G, Fiorillo E, Ganora D, Housseini IM, Katiellou GL, Piras M, Tarchiani V (2025) Flood damage risk mapping along the River Niger: ten benefits of a participated approach. Climate (Basel) 13:80. https://doi.org/10.3390/cli13040080

United Nations General Assembly (2023). Main findings and recommendations of the midterm review of the implementation of the Sendai framework for disaster risk reduction 2015–2030. 31 January 2023 A/77/640. https://documents.un.org/doc/undoc/gen/n22/764/26/pdf/n2276426.pdf (Accessed on 15/6/2025)

United Nations (2015) Sendai framework for disaster risk reduction 2015–2030, Geneva (Switzerland), UNDRR

Ward PJ, Jongman B, Sperna Weiland F, Bouwman A, van Beek R, Bierkens MFP, Ligtvoet W, Winsemius HC (2013) Assessing flood risk at the global scale: model setup, results, and sensitivity. Environ Res Lett 8:044019. https://doi.org/10.1088/1748-9326/8/4/044019

Publisher's Note Springer Nature remains neutral with regard to jurisdictional claims in published maps and institutional affiliations.